Nicolson-Ross-Weir (NRW) and Baker-Jarvis Algorithms

(13)-(15)

Equations (4) & (5) and ^{V} from the last lecture can be used to extract the material parameters of the specimen. We'll discuss two approaches for extracting material parameters using reflection and transmission data.

1. Nicolson-Ross-Weir (NRW) algorithm. In this algorithm, the measured S parameters at the specimen faces are used to determine ϵ & μ. From (4) & (5) in the previous lecture

$$S_{11} = \frac{\Gamma_p(1-P^2)}{1-\Gamma_p^2 P^2} = S_{22} \tag{1}$$

&

$$S_{21} = \frac{P(1-\Gamma_p^2)}{1-\Gamma_p^2 P^2} = S_{12} \tag{2}$$

These S parameters are equated to those measured at the sample faces. That is,

$$S_{11}^{m'} = \frac{\Gamma_p(1-P^2)}{1-\Gamma_p^2 P^2} = S_{22}^{m'} \tag{3}$$

and

$$S_{21}^{m'} = \frac{P(1-\Gamma_p^2)}{1-\Gamma_p^2 P^2} = S_{12}^{m'} \tag{4}$$

Following Nicolson-Ross and Weir, these two eqns. can be combined to yield

$$\Gamma_p = X \pm \sqrt{X^2-1} \tag{5}$$

where $$X = \frac{(S_{11}^{m'})^2 - (S_{21}^{m'})^2 + 1}{2\,S_{11}^{m'}} \tag{6}$$

the sign in (5) is chosen so that $|\Gamma_p| \leq 1$.

Further, from (3)-(5) an expression for P can be found as

$$P = \frac{S_{11}^{m\prime} + S_{21}^{m\prime} - \Gamma_p}{1 - (S_{11}^{m\prime} + S_{21}^{m\prime})\Gamma_p} \tag{7}$$

The RHS's of (5) & (7) are <u>numbers</u> computed from measured data. The LHS's of (6) & (7) are directly related to the specimen's material parameters. We defined in the last lecture that

$$\frac{\eta_r - 1}{\eta_r + 1} = \Gamma_p \tag{8}$$

and

$$e^{-\gamma L} = P \tag{9}$$

where $\eta_r = \sqrt{\frac{\epsilon_r}{\mu_r}}$ and $\gamma = j\omega\sqrt{\mu\epsilon} = \gamma_0\sqrt{\mu_r\epsilon_r}$ (10),(11)
with $\gamma_0 = j\omega\sqrt{\mu_0\epsilon_0}$ (12)

Using (10) & (11) in (8) & (9) the relative material parameters of the MUT are

$$\mu_r = \frac{1+\Gamma_p}{(1-\Gamma_p)\Lambda/\lambda_0} = \frac{\lambda_0}{\Lambda}\,\frac{1+\Gamma_p}{1-\Gamma_p} \tag{13}$$

&

$$\epsilon_r = \frac{\lambda_0^2}{\mu_r\Lambda^2} \tag{14}$$

Text equation is incorrect, even for $\lambda_c \to \infty$.

where λ_o = free space wavelength and

$$\frac{1}{\Lambda^2} = \frac{\epsilon_r \mu_r}{\lambda_o^2} = -\left[\frac{1}{2\pi L} \ln\left(\frac{1}{P}\right)\right]^2 \qquad (15)$$

Because P is a complex number, we must be careful when computing the natural logarithm. In general,

$$\ln \frac{1}{P} = Ln \frac{1}{|P|} + j\left[Arg\left(\frac{1}{P}\right) + n 2\pi\right] \qquad (16)$$

$$\text{for} \quad n = 0, \pm 1, \pm 2, \ldots$$

and $Arg\left(\frac{1}{P}\right)$ is the principal value s.t. $-\pi < Arg\left(\frac{1}{P}\right) \le \pi$.

The proper choice for n in (16) is determined by equating the predicted time delay through the specimen to the time delay computed from measured data. This ambiguity arises because the phase angle of the propagation factor P is unchanged when the sample length is increased by a multiple of a wavelength.

Another technique to determining the proper n in (16) is to use a technique called "phase-unwrapping", as discussed in the text (pp. 177-178).

Example from: - Baker Jarvis. PTFE.
- Weir - PTFE

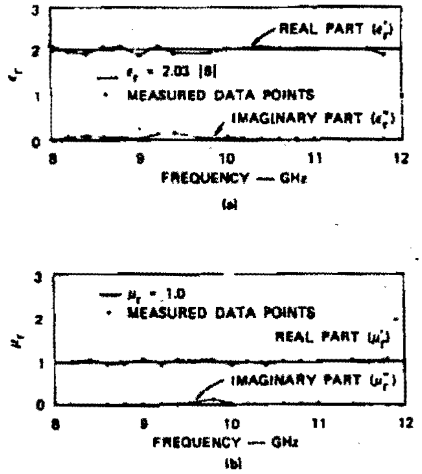

Fig. 2. Measured dielectric constant and permeability of Teflon in the X-band region. (a) Relative dielectric constant (ϵ_r). (b) Relative permeability (μ_r).

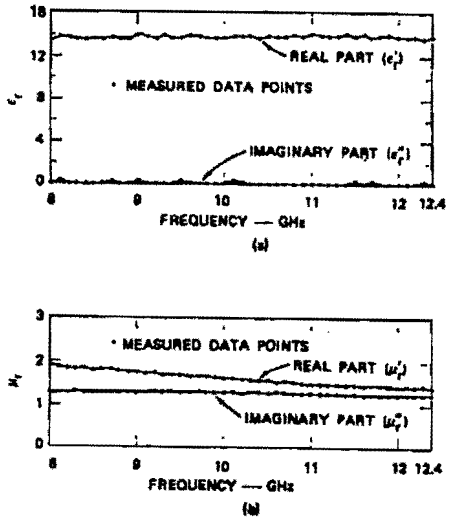

Fig. 3. Measured dielectric constant and permeability of Eccosorb SF-5.5 in the X-band region. (a) Relative dielectric constant (ϵ_r). (b) Relative permeability (μ_r).

Reference: W. B. Weir, "Automatic measurement of complex dielectric constant and permeability at microwave frequencies," *Proc. IEEE*, vol. 62, no. 1, pp. 33-36, 1974.

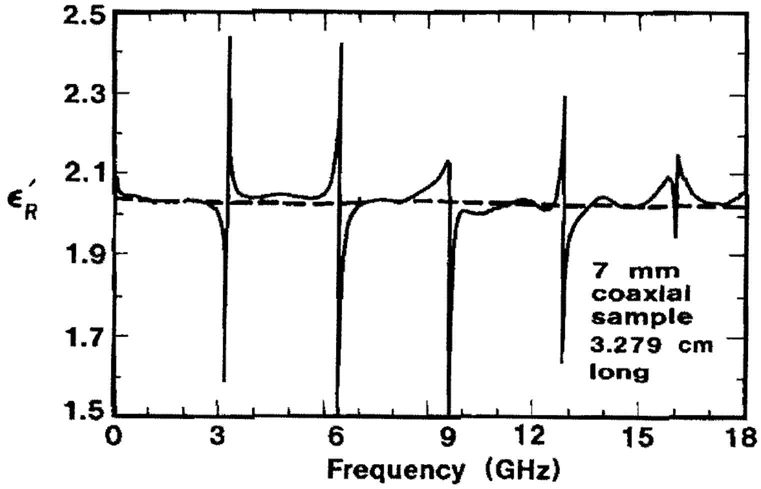

Fig. 2. The determination of the permittivity of a PTFE sample as a function of frequency using the Nicolson and Ross equations (solid line) and the iteration procedure (dashed line) (eq. (21)).

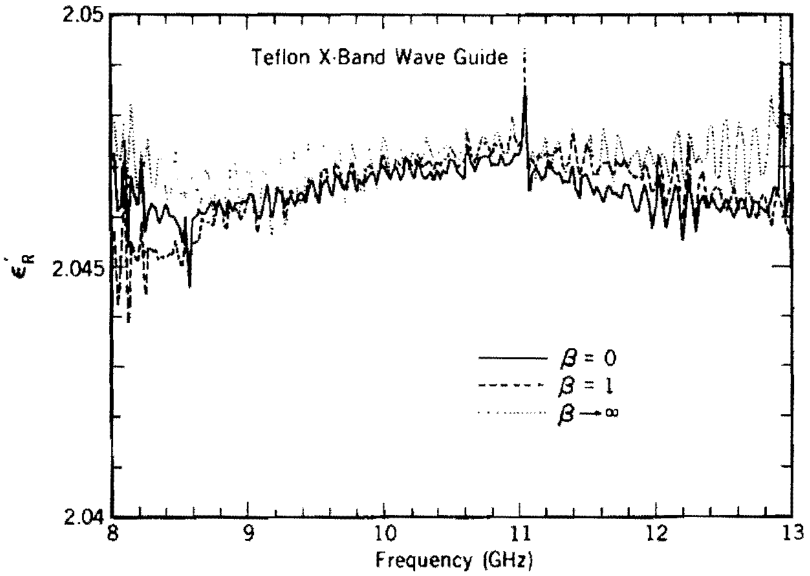

Fig. 3. The permittivities obtained from (24) for various values of β for a sample of PTFE. The dashed line is for $\beta \to \infty$, the solid line for $\beta = 0$, and the dotted line for $\beta = 1$.

Reference: J. Baker-Jarvis, E. J. Vanzura and W. A. Kissick, "Improved technique for determining complex permittivity with the transmission/reflection method," *IEEE Trans. Microwave Theory Tech.*, vol. 38, no. 8, pp. 1096-1103, 1990.

Weir's results for Teflon show more freq. variation and error than expected. He reports this was likely due to the lack of freq. stabilization in the network analyzer, which was present for the Eccosorb SF-5.5 measurements.

The Teflon results from Baker-Jarvis show many peaks and large errors. These occur when specimen is an integer # of half-wavelengths long in the specimen. Why not peaks in Weir data? Specimen was 1" long. ($\lambda/2 = 0.0254$ m $\Rightarrow f_{\lambda/2} = 4.14$ GHz for TEM. But his measurements in rectangular waveguide. λ_g different.) Baker-Jarvis's measurements in air-line fixture (TEM) with a relatively long specimen = 3.279 cm ($\lambda/2 = 0.03279 \Rightarrow f_{\lambda/2} \approx 3.21$ GHz.)

Boughriet, et al., attribute this error in the NRW algorithm to the term $\frac{1+\Gamma_p}{1-\Gamma_p}$ in (13) and $\frac{1-\Gamma_p}{1+\Gamma_p}$ in (14).

Otherwise, all calc. in NRW in (5), (6), (7) are not prone to this error.

2. <u>Baker-Jarvis Method</u>. In this algorithm, a set of equations is solved numerically using a root-finding or estimation method. Not an explicit solution for ϵ & μ but doesn't suffer from numerical instabilities at freq. where specimen length is multiple number of half-wavelengths.

In a typical Baker-Jarvis algorithm application, the material parameters are unknown, as well as the specimen length L, and the specimen location in the holder, R_1 & R_2. That's seven unknowns, where $R_{\frac{1}{2}} \equiv e^{-\gamma_0 L_{\frac{1}{2}}}$

Baker-Jarvis, et al show a number of equations that are not dependent on the location of the specimen, i.e., so-called reference plane independent expressions.

For example, from $S_{11}^m = R_1^2 \dfrac{\Gamma_p (1-P^2)}{1-\Gamma_p^2 P^2}$ then,

$$|S_{11}^m| = \left| \frac{\Gamma_p (1-P^2)}{1-\Gamma_p^2 P^2} \right| \quad (17)$$

Which is not dependent on R_1.

Other reference plane independent expressions can be found in (18)-(21) of Baker-Jarvis et al.

As mentioned previously, grab as many of these reference-plane independent expressions as # of unknowns. Use numerical methods to solve for unknowns.

...A techniques of combining linear combinations of the
...reference-plane independent expressions proposed by Baker-Jarvis
...et al, has become quite popular. In particular, (3) is
...added to $\beta \cdot (4)$, where β is a real number as:

$$\frac{1}{2}\left[S_{12}^{m'}+S_{21}^{m'}+\beta\left(S_{11}^{m'}+S_{22}^{m'}\right)\right]=\frac{P(1-\Gamma_p^2)+\beta\Gamma_p(1-P^2)}{1-\Gamma_p^2 P^2} \qquad (18)$$

...The parameter β is chosen to weight the reflection
...measurements more if lo-reflect is small, or large
...to weight reflect meas. more if Transmission small.

[Show Fig 3, Baker-Jarvis]

To further illustrate the usefulness of the Baker-Jarvis paper, imagine a situation when measuring the "effective" permittivity of particulate media, such as this configuration:

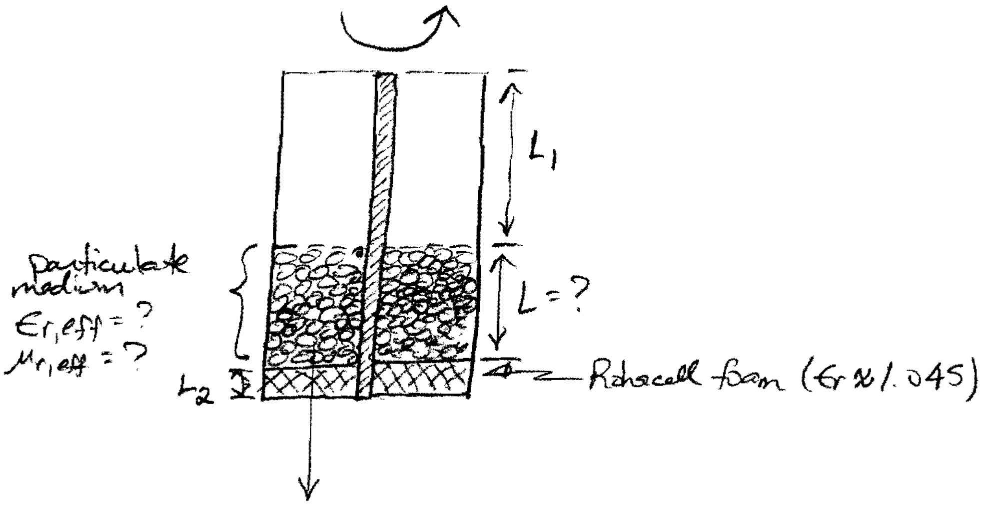

The specimen thickness and position in the fixture may not be known, or known to a necessary precision. Other examples include

- Liquids - can't see into fixture, or measure "nondestructively"
- Compressible specimens - butter-like materials, etc. With a composite material such as titanate in polymer, $\epsilon_{r,eff}$ will change when compressed. For solids, ϵ_r won't change, but still need accurate specimen dimensions for accurate ϵ_r.

In such cases where L may not be known as well as perhaps L_1, Baker-Jarvis et al. suggest combining

$$S_{21}S_{12} - S_{11}S_{22} = e^{-2\gamma_0 (L_{air}-L)} \frac{z^2-\Gamma^2}{1-z^2\Gamma^2} \quad (21), \quad z \equiv e^{-\gamma L}$$

w/ their (17)-(20) to treat the measurement as independent of reference plane and specimen thickness. Neat!